A Mathematical Model of Action Potential in Rat Atrial Cells

Na Zhao[1], Yimei Du[3], Kuanquan Wang[1], Henggui Zhang[1,2], Qince Li[1]

[1]School of Computer Science and Technology, Harbin Institute of Technology, Harbin, China
[2]School of Physics and Astronomy, University of Manchester, Manchester, UK
[3]Wuhan Union Hospital, Tongji Medical College of Huazhong University of Science and Technology, Wuhan, China

Abstract

Atrial fibrillation (AF) is a common cardiac arrhythmia associated with cardiac morbidity and mortality. Though several computational models have been developed to investigate mechanisms of atrial fibrillation in many species, there is no such model for adult rat atrial cells. A biophysically detailed mathematical model of the action potential of the rabbit atrial cells was developed based on experimental data recorded from rat right atrial cells. Conductance of I_{to}, I_{Kur}, I_{Kr}, I_{Ks}, I_{K1} as well as the time constant of I_{to} activation (τ_s) were modified to fit I-V curve of potassium current. Conductance, voltage dependent activation and inactivation of I_{CaL} were modified to fit I-V, activation and inactivation curves of I_{CaL} current. I-V, activation and inactivation curves of I_{Na} current were fitted similarly. The action potential from the computational model are comparable to the action potential (AP) recorded from rat atrial cells. The resting membrane potential, action potential amplitude and APD_{50} are -67.4 mV, 80.7 mV and 18 ms, respectively. This study, for the first time, developed a computational model of action potentials of rat atrial cells. The model can be used to further explore pathological mechanisms of atrial fibrillation.

1. Introduction

Atrial fibrillation (AF) is the most common arrhythmia observed in patients [1–3], AF can be mainly classified into three types, including paroxysmal, persistent, or chronic AF. In order to design optimal treatment for each type of AF, a profound understanding of the underlying mechanisms is required. *In vivo* experiments are require to get a better understanding of the role of ion channel remodeling in AF. Practically, a more common method is to investigate the mechanisms of AF *in vitro*. However, in *vivo* and *in vitro* have several limitations despite insights of the mechanism underlying arrhythmogenesis can be provided from these approaches. For example, in *vivo* and *in vitro* studies, it is impractical to investigate the electrophysiological properties at different physical scales (from cellular level to organ level) in one experiment. The electrophysiological properties recorded form different experiments, such as path clamp and optical mapping, may be affected by gradually change in cell/tissue properties. Therefore, computer models are widely used in cardiac arrhythmia studies in basic as well as clinical researches [4-7].

In order to investigate the mechanisms of AF in rats, the basis is a detailed computational model of the action potential of the rabbit atrial cells. Although, in last few decades, a large number of computational model have been developed for different cardiac cells in different species [8-13], a mathematical model for the adult rat atrial myocyte is still lacking.

In this study, we developed the first mathematical model for adult rat atrial cells, based on experimental data. The parameters of sodium, calcium and potassium current were adjusted to fit the experimental data obtained from patch clamp. The simulation results demonstrate that I-V, activation and inactivation curves of calcium, sodium and potassium currents are consistent with experimental data from the rat atrial cells. Also, the profile of simulated AP is consistent with experimental data.

2. Methods

The patch clamp data are provided by Du *et al*. Rat atrial myocytes were patch-clamped using the whole-cell technique at 20–23°C.

The cell membrane of the rat atrial myocytes was mimicked as an electrical circuit. The action potential behavior in a rat atrial myocyte was calculated by the following ordinary differential equation (Eq. 1),

$$C_m \frac{dV}{dt} = -I_{ion} + I_{stim}, \quad (1)$$

where C_m is the cell capacitance, V is the transmembrane voltage, t is time, I_{ion} is the total transmembrane ionic

current, and I_{stim} is the stimulus current.

The total transmembrane ionic current (I_{tot}) was calculated as the summation of the fast Na^+ current (I_{Na}), the L-type Ca^{2+} current (I_{CaL}), the transient outward K^+ current (I_{to}), the rapidly activating K^+ current (I_{Kr}), the slow activating K^+ current (I_{Ks}), the inward-rectifier K^+ current (I_{K1}), the ultra-rapid delayed rectifier outward K^+ current (I_{Kur}), the Ca^{2+}-activated Cl^- current (I_{ClCa}), the Na^+/Ca^{2+} exchanger current (I_{NaCa}), the Na^+/K^+ pump current (I_{NaK}), Na^+/K^+ pump current (I_{NaK}), the sarcolemmal Ca pump current (I_{pCa}) and the background current (I_b) as shown in Eq.2.

$$I_{tot} = I_{Na} + I_{Ca} + I_{to} + I_{Kr} + I_{Ks} + I_{K1} + I_{Kur} + I_{ClCa} + I_{CaNa} + I_{NaK} + I_{pCa} + I_b \quad (2)$$

The current model was based on the model of human atrial cell developed by Grandi *et al* in 2011 [9]. The plateau K^+ current (I_{kp}) in Grandi's model was removed and the ultra-rapid delayed rectifier outward K^+ current (I_{Kur}) developed by Maleckar *et al* in 2009 [10] was added into the current model. The formulas of I_{to}, I_{Kr}, I_K and I_{K1} in Grandi's model were replaced with those developed by *Majumder et al* in 2016 [11]. The formulas of fast Na^+ current in Grandi's model were replaced with those developed by *ten* Tusscher *et al* in 2004 [12]. In order to reproduce the action potential of adult rat atrial cells, parameters of potassium, sodium and calcium ionic channels were modified to fit the experimental data.

3. Results

3.1. K^+ currents

In our model, as the main repolarization component, potassium current (I_K) is consist of the I_{to}, I_{Kr}, I_{Ks}, I_{K1}, and I_{Kur} as shown in Eq.3.

$$I_K = I_{to} + I_{Kr} + I_{Ks} + I_{K1} + I_{Kur} \quad (3)$$

Although it has been reported that I_{to} has two components that can rapidly and slowly recover from inactivation ($I_{to,f}$ and $I_{to,s}$), in adult rat atrial cells, only $I_{to,f}$ were observed in several studies. Therefore, only $I_{to,f}$ current was calculated in current model.

The total potassium current was fitted with voltage clamp experimental data in rat right atrial cells. During the voltage clamp, the voltage was hold at -40ms for 110ms in the beginning and then clamped to a series of testing potential ranging from -90mV to 40mV with a step of 10mV for 500ms.

The conductance of the transient outward K^+ current (G_{to}), rapidly activating K^+ current (G_{Kr}), slow activating K^+ current (G_{Ks}), inward-rectifier K^+ current (G_{K1}), ultra-rapid delayed rectifier outward K^+ current (G_{Kur}) as well as time constant of I_{to} inactivation (τ_{ytof}) were adjusted to fit the peak and tail total potassium current from experimental data. The adjusted parameters and equations are listed in Tab. 1 and Eq. 4.

Table 1. Values of parameters of potassium currents.

Parameters	Value	Unit
G_{to}	0.48	mS/μF
G_{Kur}	0.0363	mS/μF
G_{Kr}	0.01135	mS/μF
G_{Ks}	0.0866	mS/μF
G_{K1}	7. 48	mS/μF

$$\tau_{ytof} = 0.35 \cdot e^{-\left(\frac{V_m+70}{15}\right)^2+0.035} - 15.64 \quad (4)$$

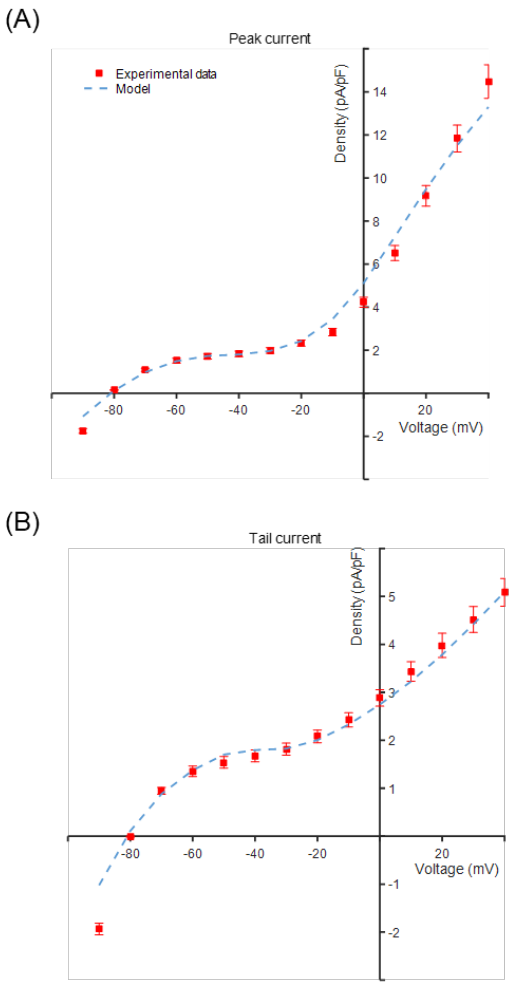

Figure 1. Data fitting of total potassium current.

The fitting results of peak and tail total potassium current are shown in Figure 1A and 1B, respectively. The I-V curves of peak and tail current had a similar profile. In the range from -80mV to -60mV and from -20mV to 40mV,

both peak and tail currents increased significantly. However, in the range from -60mV to -20mV, no significant change was observed in both curves. The simulation results were mainly consistent with experimental data in spite of a decline at -90mV.

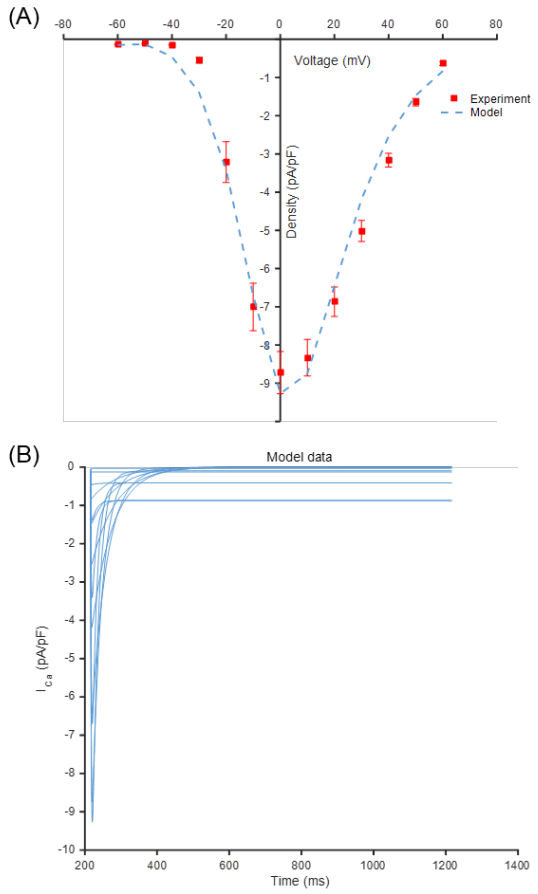

Figure 2. Reproduced I-V relationship (A) and the current traces (B) of I_{CaL} during voltage clamp.

3.2. L-type Ca^{+} current

The permeability (P_{Ca}) and steady state voltage-dependent activation (d_{ss}), steady state voltage-dependent inactivation (f_{ss}) and time constant of voltage-dependent inactivation (τ_f) of L-type Ca^{2+} current were modified to reproduce the I-V curve of I_{CaL} measured in patch clamp.

The permeability was increased by 2.35-folds to reproduce I_{CaL} amplitude. The detailed modifications of gating variables of I_{CaL} are shown in Eq.5-7.

$$d_{ss} = 1 - \frac{1}{1 + e^{\left(\frac{V+8.85784}{6.60054}\right)}}, \tag{5}$$

$$f_{ss} = \frac{1}{1 + e^{\left(\frac{V+29.77913}{6.01471}\right)}}, \tag{6}$$

$$\tau_f = \frac{14.1}{1 + e^{\left(-\frac{(V+20.0)^2}{800}+0.2\right)}}. \tag{7}$$

The fitting results of L-type Ca^{2+} current are shown in Figure 2. The simulated I-V curve of I_{CaL} showed a bell shape with a peak value of ~9.2pA/pF at 0mV which is consistent with experimental data. In the simulation, the current density dropped a little faster than experimental recording at the range from -50mV to -20mV (Fig. 2A). Figure 2B demonstrated the simulated time traces of I_{CaL} during voltage clamp. The results agree with the experimental recording as well (data not shown).

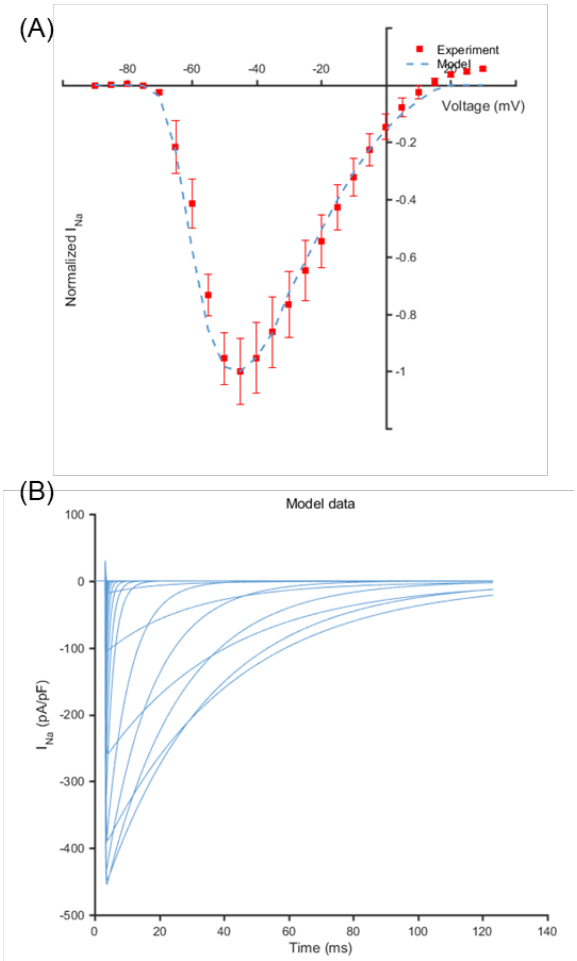

Figure 3. Normalized I-V relationship (A) and the current traces (B) of I_{Na} during voltage clamp.

3.3. Fast Na^{+} current

The formulas of I_{Na} was based on the model developed by *ten* Tusscher *et al*. The steady state activation (m_{ss}), time constant of activation (τ_m), steady state fast inactivation (h_{ss}) , time constant of fast activation (τ_h), steady state slow inactivation (j_{ss}) and time constant of slow activation

(τ_j) were modified to fit the experimental data and produce the upstroke of action potential.

The fitting results of fast Na^+ current are shown in Figure 3. The simulated I-V curve of I_{Na} showed a bell shape with a peak value ~450pA/pF at -45mV which is consistent with experimental data (Fig. 3A). Figure 3B demonstrated the simulated time traces of I_{Na} during voltage clamp.

3.4. Action potential

The action potential was produced by applying a series of 1Hz external stimuli with the amplitude -80pA/pF of and the duration of 1ms. The time trace of simulated AP is presented in Figure 4. The resting membrane potential, action potential amplitude and APD_{50} were measured as -67.4 mV, 80.7 mV and 18 ms, respectively.

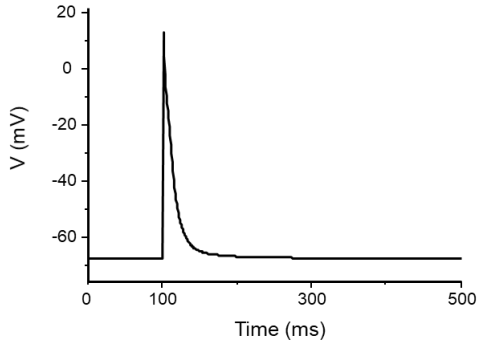

Figure 4. The simulated action potential at 1 Hz.

4. Conclusion

In this study, we developed the first adult rat atrial computational model based on experimental data. The simulation results are consistent with experimental recordings. Development of such model is crucial since it would allow researchers to compare the results obtained *in vivo*/*in vitro* studies with the simulation results obtained *in silico* simulations.

Acknowledgments

The work is supported by the National Nature Science Foundation of China (NSFC) (No. 61601143, 81770328, 61572152, and 61571165), Heilongjiang and China Postdoctoral Science Foundation under Grant nos.2015M581448 (to QL), the Natural Science Foundation of Shandong Province (No. ZR2017MF051), the Science Technology and Innovation Commission of Shenzhen Municipality (No. JSGG20160229125049615 and JCYJ20151029173639477).

References

[1] C. R. Wyndham. "Atrial fibrillation: the most common arrhythmia," *Tex. Heart I. J.*, vol. 27, no. 3, pp. 257–267, Feb. 2000.

[2] M. C. Wijffels, C. J. Kirchhof, R. Dorland, J. Power, M. A. Allessie. "Electrical remodeling due to atrial fibrillation in chronically instrumented conscious goats - Roles of neurohumoral changes, ischemia, atrial stretch, and high rate of electrical activation" *Circulation*, vol. 96, no. 10, pp. 3710–3720, Nov. 1997.

[3] M. A. Allessie, "Atrial electrophysiologic remodeling: Another vicious circle?" *J. Cardiovasc. Electr.,* vol. 9, no. 12, pp. 1378–1393, Dec. 1998.

[4] Z. L. Qu et al, "Scroll wave dynamics in a three-dimensional cardiac tissue model: roles of restitution, thickness, and fiber rotation," *Biophys. J.*, vol. 78, no. 6, pp. 2761– 2775, Jun. 2000.

[5] R. Majumder, A. R. Nayak, R. Pandit, "Scroll-wave dynamics in human cardiac tissue: lessons from a mathematical model with inhomogeneities and fiber architecture," *PLoS One*, vol. 6, no. 4, Apr. 2011, Art. no. e18052.

[6] P. M .Boyle et al, "Purkinje-mediated effects in the response of quiescent ventricles to defibrillation shocks," *Ann. Biomed. Eng.*, vol. 38, no. 2, pp. 456– 468, Feb. 2010.

[7] N. Trayanova, J. Eason, F. Aguel, "Computer simulations of cardiac defibrillation: a look inside the heart," *Computing and Visualization in Science*, vol. 4, no. 4, pp. 259– 270, Jul. 2002.

[8] E. Grandi, F. S. Pasqualini, D. M. Bers, "A novel computational model of the human ventricular action potential and Ca transient," *J. Mol. Cell. Cardiol.*, vol. 48, no. 1, pp. 112– 121, Jan. 2010.

[9] E. Grandi et al, "Human atrial action potential and Ca^{2+} model: sinus rhythm and chronic atrial fibrillation," *Circulation*, vol. 109, no. 9, pp. 1055– 1066, Oct. 2011.

[10] M. M. Maleckar et al, "K^+ current changes account for the rate dependence of the action potential in the human atrial myocyte," *Am. J. Physiol.-Heart C.*, vol. 297, no. 4, pp. H1398-H1410, Oct. 200p.

[11] R. Majumder et al, "A mathematical model of neonatal rat atrial monolayers with constitutively active acetylcholine-mediated K+ current," *PLoS Comput. Biol.*, vol. 12, no. 6, Jun. 2016, Art. no. e1004946.

[12] K. ten Tusscher et al, "A model for human ventricular tissue," *Am. J. Physiol.-Heart C.*, vol. 286, no. 4, pp. H1573-H1589, Apr. 2004.

[13] H. Zhang et al, "Mathematical models of action potentials in the periphery and center of the rabbit sinoatrial node," *Am. J. Physiol.-Heart C.*, vol. 279, no. 1, pp. H397-H421, Jul. 2000.

Address for correspondence

Qince Li
Xinjishu Building 901,
Harbin Institute of Technology
Xidazhi Street, Nangang District,
Harbin,
China

qinceli@hit.edu.cn